

Particle-Species Dependent Modification of Jet-Induced Correlations in Au + Au Collisions at $\sqrt{s_{NN}} = 200$ GeV

S. Afanasiev,¹⁷ C. Aidala,⁷ N. N. Ajitanand,⁴³ Y. Akiba,^{37,38} J. Alexander,⁴³ A. Al-Jamel,³³ K. Aoki,^{23,37} L. Aphecetche,⁴⁵ R. Armendariz,³³ S. H. Aronson,³ R. Averbek,⁴⁴ T. C. Awes,³⁴ B. Azmoun,³ V. Babintsev,¹⁴ A. Baldisseri,⁸ K. N. Barish,⁴ P. D. Barnes,²⁶ B. Bassalleck,³² S. Bathe,⁴ S. Batsouli,⁷ V. Baublis,³⁶ F. Bauer,⁴ A. Bazilevsky,³ S. Belikov,^{3,16} R. Bennett,⁴⁴ Y. Berdnikov,⁴⁰ M. T. Bjornedal,⁷ J. G. Boissevain,²⁶ H. Borel,⁸ K. Boyle,⁴⁴ M. L. Brooks,²⁶ D. S. Brown,³³ D. Bucher,²⁹ H. Buesching,³ V. Bumazhnov,¹⁴ G. Bunce,^{3,38} J. M. Burward-Hoy,²⁶ S. Butsyk,⁴⁴ S. Campbell,⁴⁴ J.-S. Chai,¹⁸ S. Chernichenko,¹⁴ J. Chiba,¹⁹ C. Y. Chi,⁷ M. Chiu,⁷ I. J. Choi,⁵² T. Chujo,⁴⁹ V. Cianciolo,³⁴ C. R. Cleven,¹² Y. Cobigo,⁸ B. A. Cole,⁷ M. P. Comets,³⁵ P. Constantin,¹⁶ M. Csanád,¹⁰ T. Csörgő,²⁰ T. Dahms,⁴⁴ K. Das,¹¹ G. David,³ H. Delagrange,⁴⁵ A. Denisov,¹⁴ D. d'Enterria,⁷ A. Deshpande,^{38,44} E. J. Desmond,³ O. Dietzsch,⁴¹ A. Dion,⁴⁴ J. L. Drachenberg,¹ O. Drapier,²⁴ A. Drees,⁴⁴ A. K. Dubey,⁵¹ A. Durum,¹⁴ V. Dzhordzhadze,⁴⁶ Y. V. Efremenko,³⁴ J. Egdemir,⁴⁴ A. Enokizono,¹³ H. En'yo,^{37,38} B. Espagnon,³⁵ S. Esumi,⁴⁸ D. E. Fields,^{32,38} F. Fleuret,²⁴ S. L. Fokin,²² B. Forestier,²⁷ Z. Fraenkel,^{51,*} J. E. Frantz,⁷ A. Franz,³ A. D. Frawley,¹¹ Y. Fukao,^{23,37} S.-Y. Fung,⁴ S. Gadrat,²⁷ F. Gastineau,⁴⁵ M. Germain,⁴⁵ A. Glenn,⁴⁶ M. Gonin,²⁴ J. Gosset,⁸ Y. Goto,^{37,38} R. Granier de Cassagnac,²⁴ N. Grau,¹⁶ S. V. Greene,⁴⁹ M. Grosse Perdekamp,^{15,38} T. Gunji,⁵ H.-Å. Gustafsson,²⁸ T. Hachiya,^{13,37} A. Hadj Henni,⁴⁵ J. S. Haggerty,³ M. N. Hagiwara,¹ H. Hamagaki,⁵ H. Harada,¹³ E. P. Hartouni,²⁵ K. Haruna,¹³ M. Harvey,³ E. Haslum,²⁸ K. Hasuko,³⁷ R. Hayano,⁵ M. Heffner,²⁵ T. K. Hemmick,⁴⁴ J. M. Heuser,³⁷ X. He,¹² H. Hiejima,¹⁵ J. C. Hill,¹⁶ R. Hobbs,³² M. Holmes,⁴⁹ W. Holzmann,⁴³ K. Homma,¹³ B. Hong,²¹ T. Horaguchi,^{37,47} M. G. Hur,¹⁸ T. Ichihara,^{37,38} K. Imai,^{23,37} M. Inaba,⁴⁸ D. Isenhower,¹ L. Isenhower,¹ M. Ishihara,³⁷ T. Isobe,⁵ M. Issah,⁴³ A. Isupov,¹⁷ B. V. Jacak,^{44,†} J. Jia,⁷ J. Jin,⁷ O. Jinnouchi,³⁸ B. M. Johnson,³ K. S. Joo,³⁰ D. Jouan,³⁵ F. Kajihara,^{5,37} S. Kametani,^{5,50} N. Kamihara,^{37,47} M. Kaneta,³⁸ J. H. Kang,⁵² T. Kawagishi,⁴⁸ A. V. Kazantsev,²² S. Kelly,⁶ A. Khanzadeev,³⁶ D. J. Kim,⁵² E. Kim,⁴² Y.-S. Kim,¹⁸ E. Kinney,⁶ A. Kiss,¹⁰ E. Kistenev,³ A. Kiyomichi,³⁷ C. Klein-Boesing,²⁹ L. Kochenda,³⁶ V. Kochetkov,¹⁴ B. Komkov,³⁶ M. Konno,⁴⁸ D. Kotchetkov,⁴ A. Kozlov,⁵¹ P. J. Kroon,³ G. J. Kunde,²⁶ N. Kurihara,⁵ K. Kurita,^{39,37} M. J. Kweon,²¹ Y. Kwon,⁵² G. S. Kyle,³³ R. Lacey,⁴³ J. G. Lajoie,¹⁶ A. Lebedev,¹⁶ Y. Le Bornec,³⁵ S. Leckey,⁴⁴ D. M. Lee,²⁶ M. K. Lee,⁵² M. J. Leitch,²⁶ M. A. L. Leite,⁴¹ H. Lim,⁴² A. Litvinenko,¹⁷ M. X. Liu,²⁶ X. H. Li,⁴ C. F. Maguire,⁴⁹ Y. I. Makdisi,³ A. Malakhov,¹⁷ M. D. Malik,³² V. I. Manko,²² H. Masui,⁴⁸ F. Matathias,⁴⁴ M. C. McCain,¹⁵ P. L. McGaughey,²⁶ Y. Miake,⁴⁸ T. E. Miller,⁴⁹ A. Milov,⁴⁴ S. Mioduszewski,³ G. C. Mishra,¹² J. T. Mitchell,³ D. P. Morrison,³ J. M. Moss,²⁶ T. V. Moukhanova,²² D. Mukhopadhyay,⁴⁹ J. Murata,^{39,37} S. Nagamiya,¹⁹ Y. Nagata,⁴⁸ J. L. Nagle,⁶ M. Naglis,⁵¹ T. Nakamura,¹³ J. Newby,²⁵ M. Nguyen,⁴⁴ B. E. Norman,²⁶ A. S. Nyanin,²² J. Nystrand,²⁸ E. O'Brien,³ C. A. Ogilvie,¹⁶ H. Ohnishi,³⁷ I. D. Ojha,⁴⁹ H. Okada,^{23,37} K. Okada,³⁸ O. O. Omiwade,¹ A. Oskarsson,²⁸ I. Otterlund,²⁸ K. Ozawa,⁵ D. Pal,⁴⁹ A. P. T. Palounek,²⁶ V. Pantuev,⁴⁴ V. Papavassiliou,³³ J. Park,⁴² W. J. Park,²¹ S. F. Pate,³³ H. Pei,¹⁶ J.-C. Peng,¹⁵ H. Pereira,⁸ V. Peresedov,¹⁷ D. Yu. Peressounko,²² C. Pinkenburg,³ R. P. Pisani,³ M. L. Purschke,³ A. K. Purwar,⁴⁴ H. Qu,¹² J. Rak,¹⁶ I. Ravinovich,⁵¹ K. F. Read,^{34,46} M. Reuter,⁴⁴ K. Reygers,²⁹ V. Riabov,³⁶ Y. Riabov,³⁶ G. Roche,²⁷ A. Romana,^{24,*} M. Rosati,¹⁶ S. S. E. Rosendahl,²⁸ P. Rosnet,²⁷ P. Rukoyatkin,¹⁷ V. L. Rykov,³⁷ S. S. Ryu,⁵² B. Sahlmueller,²⁹ N. Saito,^{23,37,38} T. Sakaguchi,^{5,50} S. Sakai,⁴⁸ V. Samsonov,³⁶ H. D. Sato,^{23,37} S. Sato,^{3,19,48} S. Sawada,¹⁹ V. Semenov,¹⁴ R. Seto,⁴ D. Sharma,⁵¹ T. K. Shea,³ I. Shein,¹⁴ T.-A. Shibata,^{37,47} K. Shigaki,¹³ M. Shimomura,⁴⁸ T. Shohjoh,⁴⁸ K. Shoji,^{23,37} A. Sickles,⁴⁴ C. L. Silva,⁴¹ D. Silvermyr,³⁴ K. S. Sim,²¹ C. P. Singh,² V. Singh,² S. Skutnik,¹⁶ W. C. Smith,¹ A. Soldatov,¹⁴ R. A. Soltz,²⁵ W. E. Sondheim,²⁶ S. P. Sorensen,⁴⁶ I. V. Sourikova,³ F. Staley,⁸ P. W. Stankus,³⁴ E. Stenlund,²⁸ M. Stepanov,³³ A. Ster,²⁰ S. P. Stoll,³ T. Sugitate,¹³ C. Suire,³⁵ J. P. Sullivan,²⁶ J. Sziklai,²⁰ T. Tabaru,³⁸ S. Takagi,⁴⁸ E. M. Takagui,⁴¹ A. Taketani,^{37,38} K. H. Tanaka,¹⁹ Y. Tanaka,³¹ K. Tanida,^{37,38} M. J. Tannenbaum,³ A. Taranenko,⁴³ P. Tarján,⁹ T. L. Thomas,³² M. Togawa,^{23,37} J. Tojo,³⁷ H. Torii,³⁷ R. S. Towell,¹ V.-N. Tram,²⁴ I. Tseruya,⁵¹ Y. Tsuchimoto,^{13,37} S. K. Tuli,² H. Tydesjö,²⁸ N. Tyurin,¹⁴ C. Vale,¹⁶ H. Valle,⁴⁹ H. W. van Hecke,²⁶ J. Velkovska,⁴⁹ R. Vertesi,⁹ A. A. Vinogradov,²² E. Vznuzdaev,³⁶ M. Wagner,^{23,37} X. R. Wang,³³ Y. Watanabe,^{37,38} J. Wessels,²⁹ S. N. White,³ N. Willis,³⁵ D. Winter,⁷ C. L. Woody,³ M. Wysocki,⁶ W. Xie,^{4,38} A. Yanovich,¹⁴ S. Yokkaichi,^{37,38} G. R. Young,³⁴ I. Younus,³² I. E. Yushmanov,²² W. A. Zajc,⁷ O. Zaudtke,²⁹ C. Zhang,⁷ J. Zimányi,^{20,*} and L. Zolin¹⁷

(PHENIX Collaboration)

¹Abilene Christian University, Abilene, Texas 79699, USA

²Department of Physics, Banaras Hindu University, Varanasi 221005, India

- ³Brookhaven National Laboratory, Upton, New York 11973-5000, USA
⁴University of California–Riverside, Riverside, California 92521, USA
⁵Center for Nuclear Study, Graduate School of Science, University of Tokyo, 7-3-1 Hongo, Bunkyo, Tokyo 113-0033, Japan
⁶University of Colorado, Boulder, Colorado 80309, USA
⁷Columbia University, New York, New York 10027, USA, and Nevis Laboratories, Irvington, New York 10533, USA
⁸Dapnia, CEA Saclay, F-91191, Gif-sur-Yvette, France
⁹Debrecen University, H-4010 Debrecen, Egyetem tér 1, Hungary
¹⁰ELTE, Eötvös Loránd University, H-1117 Budapest, Pázmány P. s. 1/A, Hungary
¹¹Florida State University, Tallahassee, Florida 32306, USA
¹²Georgia State University, Atlanta, Georgia 30303, USA
¹³Hiroshima University, Kagamiyama, Higashi-Hiroshima 739-8526, Japan
¹⁴IHEP Protvino, State Research Center of Russian Federation, Institute for High Energy Physics, Protvino, 142281, Russia
¹⁵University of Illinois at Urbana-Champaign, Urbana, Illinois 61801, USA
¹⁶Iowa State University, Ames, Iowa 50011, USA
¹⁷Joint Institute for Nuclear Research, 141980 Dubna, Moscow Region, Russia
¹⁸KAERI, Cyclotron Application Laboratory, Seoul, Korea
¹⁹KEK, High Energy Accelerator Research Organization, Tsukuba, Ibaraki 305-0801, Japan
²⁰KFKI Research Institute for Particle and Nuclear Physics of the Hungarian Academy of Sciences (MTA KFKI RMKI), H-1525 Budapest 114, POBox 49, Budapest, Hungary
²¹Korea University, Seoul, 136-701, Korea
²²Russian Research Center “Kurchatov Institute,” Moscow, Russia
²³Kyoto University, Kyoto 606-8502, Japan
²⁴Laboratoire Leprince-Ringuet, Ecole Polytechnique, CNRS-IN2P3, Route de Saclay, F-91128, Palaiseau, France
²⁵Lawrence Livermore National Laboratory, Livermore, California 94550, USA
²⁶Los Alamos National Laboratory, Los Alamos, New Mexico 87545, USA
²⁷LPC, Université Blaise Pascal, CNRS-IN2P3, Clermont-Fd, 63177 Aubiere Cedex, France
²⁸Department of Physics, Lund University, Box 118, SE-221 00 Lund, Sweden
²⁹Institut für Kernphysik, University of Muenster, D-48149 Muenster, Germany
³⁰Myongji University, Yongin, Kyonggido 449-728, Korea
³¹Nagasaki Institute of Applied Science, Nagasaki-shi, Nagasaki 851-0193, Japan
³²University of New Mexico, Albuquerque, New Mexico 87131, USA
³³New Mexico State University, Las Cruces, New Mexico 88003, USA
³⁴Oak Ridge National Laboratory, Oak Ridge, Tennessee 37831, USA
³⁵IPN-Orsay, Université Paris Sud, CNRS-IN2P3, BP1, F-91406, Orsay, France
³⁶PNPI, Petersburg Nuclear Physics Institute, Gatchina, Leningrad region, 188300, Russia
³⁷RIKEN, The Institute of Physical and Chemical Research, Wako, Saitama 351-0198, Japan
³⁸RIKEN BNL Research Center, Brookhaven National Laboratory, Upton, New York 11973-5000, USA
³⁹Physics Department, Rikkyo University, 3-34-1 Nishi-Ikebukuro, Toshima, Tokyo 171-8501, Japan
⁴⁰Saint Petersburg State Polytechnic University, St. Petersburg, Russia
⁴¹Instituto de Física, Universidade de São Paulo, Caixa Postal 66318, São Paulo CEP05315-970, Brazil
⁴²System Electronics Laboratory, Seoul National University, Seoul, Korea
⁴³Chemistry Department, Stony Brook University, SUNY, Stony Brook, New York 11794-3400, USA
⁴⁴Department of Physics and Astronomy, Stony Brook University, SUNY, Stony Brook, New York 11794, USA
⁴⁵SUBATECH (Ecole des Mines de Nantes, CNRS-IN2P3, Université de Nantes) BP 20722-44307, Nantes, France
⁴⁶University of Tennessee, Knoxville, Tennessee 37996, USA
⁴⁷Department of Physics, Tokyo Institute of Technology, Oh-okayama, Meguro, Tokyo 152-8551, Japan
⁴⁸Institute of Physics, University of Tsukuba, Tsukuba, Ibaraki 305, Japan
⁴⁹Vanderbilt University, Nashville, Tennessee 37235, USA
⁵⁰Advanced Research Institute for Science and Engineering, Waseda University, 17 Kikui-cho, Shinjuku-ku, Tokyo 162-0044, Japan
⁵¹Weizmann Institute, Rehovot 76100, Israel
⁵²Yonsei University, IPAP, Seoul 120-749, Korea

(Received 18 December 2007; published 20 August 2008)

Measurements in Au + Au collisions at $\sqrt{s_{NN}} = 200$ GeV of jet correlations for a trigger hadron at intermediate transverse momentum ($p_{T,\text{trig}}$) with associated mesons or baryons at lower $p_{T,\text{assoc}}$ indicate strong modification of the away-side jet. The ratio of jet-associated baryons to mesons increases with centrality and $p_{T,\text{assoc}}$. For the most central collisions, the ratio is similar to that for inclusive measurements. This trend is incompatible with in-vacuum fragmentation but could be due to jetlike contributions from correlated soft partons, which recombine upon hadronization.

Recent measurements at the Relativistic Heavy Ion Collider (RHIC) have indicated the creation of a new state of matter in heavy-ion collisions [1]. The “soft” or small momentum transfer processes leading to the formation of this collision medium are sometimes accompanied by hard parton-parton scatterings. These scattered partons interact strongly with the medium and lose energy as they propagate through it, before fragmenting into jets [2]. This can lead to strong modification of both the yield and the angular correlation patterns of jets [3,4].

Parton energy loss in the nuclear collision medium [2] has been associated with the observation that the single particle yields of mesons (M) are significantly suppressed in Au + Au collisions, when compared to similar yields in $p + p$ collisions scaled by the number of binary nucleon-nucleon collisions [5,6]. This suppression factor R_{AA}^M decreases to ~ 0.2 for transverse momentum $p_T \gtrsim 4$ GeV/ c (in the absence of suppression, $R_{AA} = 1.0$). A general pattern of baryon (B) enhancement (for intermediate $p_T \sim 2\text{--}5$ GeV/ c) relative to mesons has been observed in central Au + Au collisions at RHIC [7,8]. No suppression is observed for $p_T \sim 1.5\text{--}4$ GeV/ c [i.e., ($R_{AA}^B \sim 1.0$)] [9], and the proton to pion ratio is observed to be about 3 times larger than in $p + p$ collisions [1].

Quark recombination [10–13] has been used to explain the enhancement of baryon emission in the intermediate p_T range. Such models also provide an explanation for the observed dependence of the elliptic flow on hadron species in terms of the “universal” elliptic flow of constituent quarks [14,15]. However, model comparisons to jetlike hadron correlation measurements [16] indicate that jet fragmentation, in concert with the recombination of thermal quarks in a flowing medium, is insufficient to account for the dihadron correlations at intermediate p_T . Thus, the search for a consistent model, which combines fragmentation and recombination dynamics to explain all of the observations in the intermediate p_T range at RHIC, remains open.

Dihadron correlation measurements have indicated suppression of the away-side jet in Au + Au collisions [17]. Recently, modifications to the distributions of the away-side jet partner hadrons measured at lower momentum have also been observed [3,4]. Indeed, these distributions show local minima at $\Delta\phi = \pi$, which contrasts with the characteristic jet peak observed in $p + p$ collisions. This modification has been attributed to strong parton-medium interactions [4,18]. A crucial question is whether or not such interactions could lead to a change in the recombination dynamics and influence the dihadron jet correlations observed at intermediate p_T .

Fries *et al.* [19,20] have argued that such a change in the recombination dynamics is to be expected from the correlations among medium partons and an energetic jet parton, induced by a “wake effect” generated by strong parton-medium interactions. That is, the energy and momentum dissipated by a hard scattered parton are absorbed by the

surrounding medium, increasing the temperature by a small amount and setting the medium into motion in the direction of the energetic parton. Thus, dihadron jet correlations could be influenced by correlated medium partons which recombine with each other or with a hard jet parton [21]. The process of recombination would also amplify these jetlike correlations for baryon creation compared to that for mesons and, hence, result in particle ratios different from the in-vacuum fragmentation values [19,21].

To gain more insight into parton-medium interactions and how they might impact recombination, we use measurements of relative azimuthal angle ($\Delta\phi$) correlation functions to make detailed investigations of the distributions and conditional yields of jet-associated baryons and mesons. Our study is made as a function of collision centrality and partner p_T , for the trigger hadron selection $2.5 < p_{T,\text{trig}} < 4.0$ GeV/ c .

Au + Au data (at $\sqrt{s_{NN}} = 200$ GeV) were recorded during 2004 with the PHENIX detector [22]. Collision centrality was determined with the beam-beam counters (BBCs) and zero degree calorimeters [22]. Charged particle tracking, identification, and momentum reconstruction in the central rapidity region ($|\eta| \leq 0.35$) was provided by two drift chambers, each with an azimuthal coverage $\Delta\varphi = \pi/2$, and two layers of multiwire proportional chambers with pad readout (PC1 and PC3). To reject most background (i.e., conversions, decays, etc.), a confirming hit was required within a 2σ matching window in PC3 [5].

Charged particles were identified via time-of-flight measurement with the time-of-flight (TOF) and lead scintillator (PbSc) detectors. The TOF covers $\Delta\varphi = \pi/4$ with good timing resolution ≈ 120 ps (see Refs. [16,23]); the PbSc as used here covers a larger solid angle ($\Delta\varphi = 3\pi/4$) with a modest timing resolution of 400 ps. The time-of-flight measurements were used in conjunction with the measured momentum and flight-path length to generate a mass-squared (m^2) distribution [24] for charged particle identification. A cut about the baryon (\bar{p} , p) peak in the m^2 distribution was used to distinguish baryons and mesons (π^\pm , K^\pm). The kaon contamination of the baryon sample is $\lesssim 3\%$ for the highest associated p_T bin used ($1.6 < p_{T,\text{assoc}}^{M,B} < 2$ GeV/ c). We generated area-normalized two-particle correlation functions, in relative azimuthal angle $C(\Delta\phi)$, as the ratio of a signal distribution $N_{\text{cor}}(\Delta\phi)$, constructed with correlated particle pairs from the same event, and a background distribution $N_{\text{mix}}(\Delta\phi)$, for pairs obtained by mixing particles from different events having similar collision vertex and centrality [3,25]:

$$C(\Delta\phi) = [N_{\text{cor}}(\Delta\phi) \int d\Delta\phi N_{\text{mix}}(\Delta\phi)] / [N_{\text{mix}}(\Delta\phi) \int d\Delta\phi N_{\text{cor}}(\Delta\phi)].$$

Representative examples of the correlation functions $[C(\Delta\phi)]$, so obtained for associated mesons and baryons ($1.3 < p_{T,\text{assoc}}^{M,B} < 1.6$ GeV/ c) per trigger hadron ($2.5 < p_{T,\text{trig}} < 4.0$ GeV/ c), are shown for two centrality selections in Fig. 1. They indicate an asymmetry characteristic

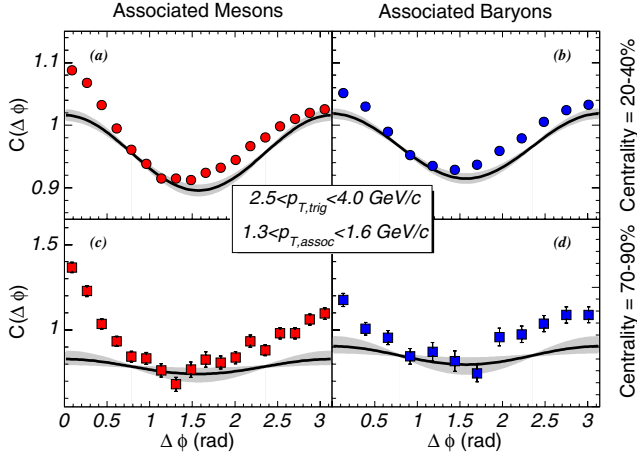


FIG. 1 (color online). Correlation functions for associated partner mesons (a),(c) and baryons (b),(d) for centrality selections of 20%–40% (top panels) and 70%–90% (bottom panels). The curves indicate elliptic flow contributions (see text).

of (di)jet-pair correlations [$J(\Delta\phi)$] and an anisotropy signaling elliptic flow [$H(\Delta\phi) = 1 + 2(v_2^{\text{trig}} \times v_2^{B,M}) \times \cos(2\Delta\phi)$] with amplitude $v_2^{\text{trig}} \times v_2^{M,B}$ [3]. The correlation functions for associated partner mesons are more asymmetric than those for associated partner baryons, indicating that the jet signal is stronger for hadron-meson correlations. However, clear separation of the jet and flow correlations is required for further study.

To extract $J(\Delta\phi)$ from $C(\Delta\phi)$, a two-source ansatz [25] is used [i.e., $C(\Delta\phi) = b_o H(\Delta\phi) + J(\Delta\phi)$]. Values for v_2^{trig} and $v_2^{M,B}$ were obtained via measurements of the single particle distributions relative to the reaction plane, determined in the BBCs [14,15]. The large (pseudo)rapidity separation ($\Delta|\eta| > 2.75$) between each BBC and the PHENIX central arms minimizes any nonflow contributions to these v_2 values [26].

To fix the value of b_o , we followed the procedure in Refs. [3,25] and assumed that $J(\Delta\phi)$ has zero yield at some minimum $\Delta\phi_{\text{min}}$ (ZYAM). That is, the elliptic flow contributions are required to coincide with $C(\Delta\phi)$ at $\Delta\phi_{\text{min}}$. Good precision for $\Delta\phi_{\text{min}}$ was achieved via a fit to the correlation function; the systematic error on the magnitude of the integrated jet function $J(\Delta\phi)$, due to the ZYAM procedure, is estimated to be $\lesssim 3\%$ from the uncertainty in setting $J(\Delta\phi) = 0$ at $\Delta\phi_{\text{min}}$. The solid lines in Fig. 1 show examples of the ZYAM-normalized elliptic flow (v_2) contributions. The gray bands represent systematic errors on the v_2 amplitudes ($\sim 6\%$ for central and midcentral events and $\sim 40\%$ for peripheral events) primarily due to an uncertainty in the reaction plane resolution [3].

The efficiency-corrected associated meson and baryon jet distributions $\frac{1}{N_{\text{trig}}} \frac{d^2 N}{dp_T d\Delta\phi}$ are shown in Fig. 2 for two associated p_T bins and for the centralities 0–20% and 20%–40%. The shaded error bars and dashed lines indicate the respective systematic error related to v_2 subtraction

and fixing b_o . The associated baryon jet-pair distributions are multiplied by the indicated factors to facilitate a shape comparison with the distributions for mesons.

Figure 2 shows that the correlation strength of the near-side jet ($\Delta\phi \leq \Delta\phi_{\text{min}}$, NS) is substantially weaker for associated baryons. In contrast, the shapes of the away-side jet distributions ($\Delta\phi \geq \Delta\phi_{\text{min}}$, AS) are qualitatively similar for associated mesons and baryons. For the central and midcentral collisions shown, these distributions are also broad and decidedly non-Gaussian, with evidence for local minima at $\Delta\phi = \pi$ [3]. They provide confirmation that the topological signatures for strong jet modification are reflected in the jet-pair distributions for both associated baryons and mesons [27]. The latter finding for baryons and mesons is an important constraint for models of strong jet modification [11,28–30].

For a given centrality and partner p_T , the integral of the extracted $J(\Delta\phi)$ distribution is the fraction of particle pairs associated with the jet, i.e., the jet-pair fraction (JPF): $\text{JPF}_{\text{NS,AS}} = \sum_{i \in \text{NS,AS}} J(\Delta\phi_i) / \sum_i C(\Delta\phi_i)$ [25]. We use it to determine the conditional yield $\langle N^{M,B} \rangle / \langle N_{\text{trig}} \rangle$, or efficiency-corrected pairs per trigger [25],

$$\frac{\langle N^{M,B} \rangle}{\langle N_{\text{trig}} \rangle} = \text{JPF} \frac{\langle N_d^{M,B} \rangle}{\langle N_s^{\text{trig}} \rangle \times \langle N_s^{M,B} \rangle} \langle N_{\text{eff}}^{M,B} \rangle,$$

where $\langle N_d^{M,B} \rangle$ is the average number of detected hadron-meson(baryon) pairs per event, $\langle N_s^{\text{trig}} \rangle$ and $\langle N_s^{M,B} \rangle$ are the detected singles rates for hadrons, mesons, and baryons, respectively, and $\langle N_{\text{eff}}^{M,B} \rangle$ are the efficiency-corrected singles rates. The systematic error associated with the latter is $\sim 10\%$. A further division by the p_T bin width gives the conditional yield $CY = \frac{1}{N_{\text{trig}}} \frac{dN}{dp_T}$, which is equivalent to an integration of the distributions shown in Fig. 2.

The conditional yields, for near- and away-side associated mesons and baryons, are shown as a function of $p_{T,\text{assoc}}$ and collision centrality in Fig. 3. The shaded error bars reflect the combined systematic error associated with

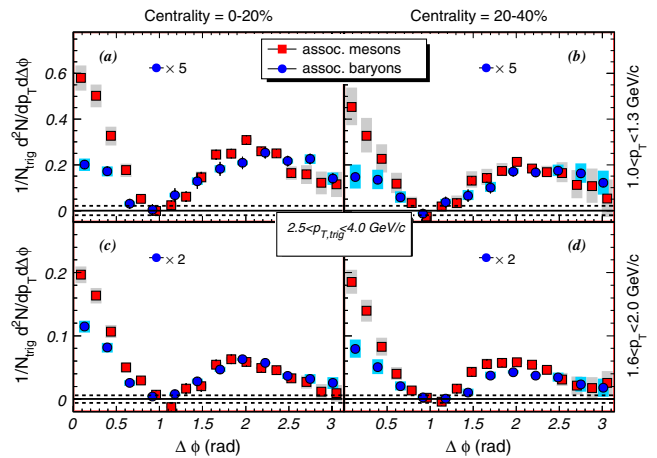


FIG. 2 (color online). Jet-pair distributions for associated mesons (squares) and baryons (circles).

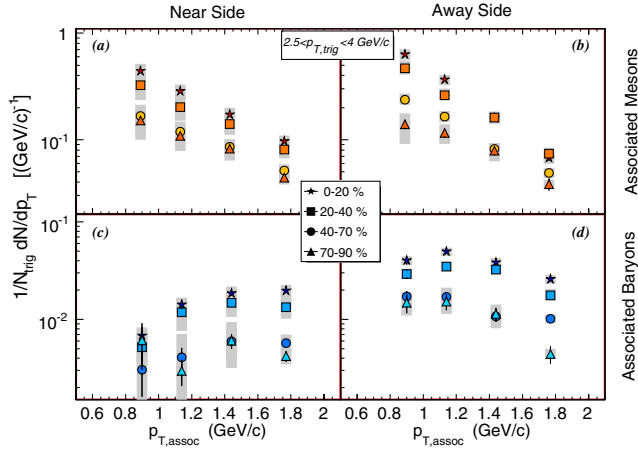


FIG. 3 (color online). Conditional jet yields for associated mesons and baryons for near-side and away-side jets.

v_2 , b_o , and the efficiency. The yields for associated mesons [Figs. 3(a) and 3(b)] indicate an essentially exponential decrease with increasing $p_{T,assoc}^M$, for both the near- and away-side jets. An increase in the inverse slope parameter T_{eff} (“temperature”) from central ($T_{eff} \sim 390$ MeV) to peripheral ($T_{eff} \sim 700$ MeV) collisions is also apparent for the away-side distributions. For a fixed $p_{T,assoc}^M$, these yields also show an increase from peripheral to central events, albeit with a stronger dependence for the away-side jet. This trend is incompatible with in-vacuum fragmentation but could be due to jetlike contributions from correlated soft partons which recombine upon hadronization [19,21], softening of the fragmentation function, and fragmentation of radiated gluons, due to energy loss [31].

The conditional yields for associated baryons differ strongly from those for associated mesons [cf. Figs. 3(c) and 3(d)]. That is, they do not show an exponential dependence on p_T^B over the measured range, and the yields for the away-side jet are substantially larger than those for the near-side jet. For a given $p_{T,assoc}^B$, the near- and away-side conditional yields increase as the collisions become more central; i.e., this trend is similar to that for the associated mesons. The baryon yields show a much stronger increase with centrality [27], as might be expected if correlated soft partons recombine and contribute to the away-side jet correlations [20].

The ratio of associated baryons to associated mesons is shown as a function of associated particle p_T in Fig. 4; the left and right panels show the ratios for the near- and away-side jets, respectively, for three centrality selections as indicated. These ratios clearly increase with p_T and with centrality for $p_T \gtrsim 1.4$ GeV/c. For peripheral collisions, the near-side ratios are qualitatively similar to the p/π ratio for jets produced in $e^+ + e^-$ collisions [32]. For more central collisions, the near- and away-side ratios are much larger, suggesting that the medium influences the relative composition of the associated particles.

The hatched bands in Fig. 4(b) show the inclusive B/M ratios (uncorrected for baryon and meson feeddown) as a

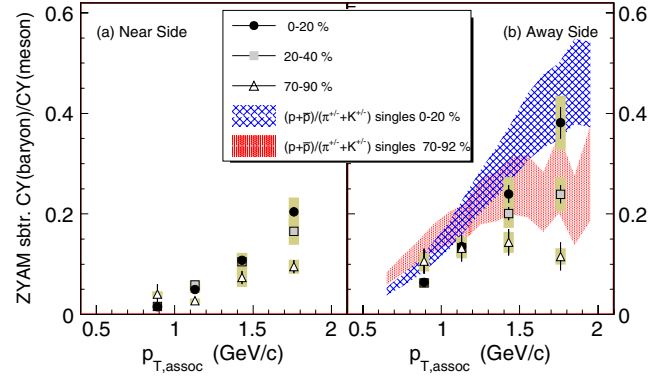


FIG. 4 (color online). Ratio of jet-associated baryons to jet-associated mesons. The hatched bands indicate inclusive B/M ratios (see text).

function of p_T for the 0–20% and 70%–92% most central Au + Au collisions [24]; an estimate of these ratios after feeddown corrections is within the systematic errors indicated by the bands. These ratios indicate that the trend of the centrality dependent baryon enhancement, apparent in the jetlike associated conditional yields, is similar to that observed for the inclusive particle yields. This suggests that the mechanisms for baryon enhancement in both the inclusive and the current away-side jet measurements have a common origin. Since recombination models can explain the enhancement of inclusive baryon yields, a qualitative explanation is that the away-side correlations result from the recombination of correlated soft partons induced via strong parton-medium interactions.

In summary, we have measured per-trigger yield distributions for jetlike associated mesons and baryons over a wide range of centrality and p_T in Au + Au collisions. The distributions for both species show similar shape modifications for the away-side jet, compatible with several jet-modification models [11,28–30]. The conditional yield distributions for mesons and baryons show different dependencies on collision centrality and associated particle p_T . The ratio of associated baryons to mesons increases with centrality and p_T , similar to the data for inclusive measurements. These results may be qualitatively understood in terms of parton-medium interactions which induce correlations between soft partons, followed by recombination at hadronization [19–21]. The observation that the baryon to meson ratio of the away-side jet approaches the ratio measured for inclusive hadrons in central Au + Au collisions suggests that the increased jetlike associated yield and large baryon to meson ratio have the same origin.

It may therefore be possible to reconcile the observed jetlike structures and the increased baryon/meson ratio at intermediate p_T in a single model for hadron production. Future quantitative model comparisons as well as measurements at higher p_T are required to fully understand the interplay between fragmentation and soft production processes.

We thank the staff of the Collider-Accelerator and Physics Departments at BNL for their vital contributions. We acknowledge support from the Office of Nuclear Physics in DOE Office of Science and NSF (USA), MEXT and JSPS (Japan), CNPq and FAPESP (Brazil), NSFC (China), IN2P3/CNRS and CEA (France), BMBF, DAAD, and AvH (Germany), OTKA (Hungary), DAE (India), ISF (Israel), KRF and KOSEF (Korea), MES, RAS, and FAE (Russia), VR and KAW (Sweden), U.S. CRDF for the FSU, U.S.–Hungarian NSF-OTKA-MTA, and U.S.–Israel BSF.

*Deceased.

†PHENIX spokesperson.

jacak@skipper.physics.sunysb.edu

- [1] K. Adcox *et al.*, Nucl. Phys. **A757**, 184 (2005).
- [2] R. Baier *et al.*, Nucl. Phys. **B483**, 291 (1997).
- [3] S. S. Adler *et al.*, Phys. Rev. Lett. **97**, 052301 (2006).
- [4] A. Adare *et al.*, Phys. Rev. C **77**, 011901 (2008).
- [5] K. Adcox *et al.*, Phys. Rev. Lett. **88**, 022301 (2001).
- [6] J. Adams *et al.*, Phys. Rev. Lett. **91**, 172302 (2003).
- [7] K. Adcox *et al.*, Phys. Rev. Lett. **88**, 242301 (2002).
- [8] C. Adler *et al.*, Phys. Rev. Lett. **89**, 092301 (2002).
- [9] S. S. Adler *et al.*, Phys. Rev. Lett. **91**, 172301 (2003).
- [10] S. A. Voloshin, Nucl. Phys. **A715**, 379 (2003).
- [11] V. Greco, C. M. Ko, and P. Levai, Phys. Rev. C **68**, 034904 (2003).
- [12] R. C. Hwa and C. B. Yang, Phys. Rev. C **67**, 034902 (2003).
- [13] R. J. Fries, B. Muller, C. Nonaka, and S. A. Bass, Phys. Rev. C **68**, 044902 (2003).
- [14] A. Adare *et al.*, Phys. Rev. Lett. **98**, 162301 (2007).
- [15] R. A. Lacey and A. Taranenko, arXiv:nucl-ex/0610029.
- [16] S. S. Adler *et al.*, Phys. Rev. C **71**, 051902 (2005).
- [17] C. Adler *et al.*, Phys. Rev. Lett. **90**, 032301 (2003).
- [18] A. Adare *et al.*, Phys. Rev. Lett. **98**, 232301 (2007).
- [19] R. J. Fries, S. A. Bass, and B. Muller, Phys. Rev. Lett. **94**, 122301 (2005).
- [20] R. J. Fries, V. Greco, and P. Sorensen, arXiv:0807.4939.
- [21] R. C. Hwa and C. B. Yang, Phys. Rev. C **70**, 024905 (2004).
- [22] K. Adcox *et al.*, Nucl. Instrum. Methods Phys. Res., Sect. A **499**, 469 (2003).
- [23] A. Adare *et al.*, Phys. Lett. B **649**, 359 (2007).
- [24] S. S. Adler *et al.*, Phys. Rev. C **69**, 034909 (2004).
- [25] N. N. Ajitanand *et al.*, Phys. Rev. C **72**, 011902(R) (2005).
- [26] J. Jia, Nucl. Phys. **A783**, 501 (2007).
- [27] The difference between the current conditional yields and those reported in Ref. [23] stem from a difference in integration range for the away-side jet.
- [28] N. Armesto, C. A. Salgado, and U. A. Wiedemann, Phys. Rev. Lett. **93**, 242301 (2004).
- [29] H. Stoecker, Nucl. Phys. **A750**, 121 (2005).
- [30] J. Casalderrey-Solana *et al.*, J. Phys. Conf. Ser. **27**, 22 (2005); Nucl. Phys. **A774**, 577 (2006).
- [31] Xin-Nian Wang, Phys. Lett. B **579**, 299 (2004).
- [32] P. Abreu *et al.*, Eur. Phys. J. C **17**, 53 (2000).